

# DECONVOLUTION OF ULTRASONIC NONDESTRUCTIVE EVALUATION SIGNALS USING HIGHER-ORDER STATISTICS

*Lahouari Ghouti, IEEE Student Member*

*Chi Hau Chen, IEEE Fellow*

Information and Computer Science Dept.  
KFUPM University  
KFUPM Box 1128, Dhahran 31261, Saudi Arabia.  
E-mail: ghouti@ccse.kfupm.edu.sa

ECE Dept.  
University of Massachusetts Darmouth  
North Darmouth, MA 02747-2300. USA.  
Email: CCHEN@umassd.edu

## ABSTRACT

In ultrasonic nondestructive evaluation (NDE) of materials, pulse echo measurements are masked by the characteristics of the measuring instruments, the propagation paths taken by the ultrasonic pulses, and are corrupted by additive noise. Deconvolution operation seeks to undo these masking effects and extract the defect impulse response which is essential for identification. In this contribution, we show that the use of higher-order statistics (HOS)-based deconvolution methods is more suitable to unravel the aforementioned effects. Synthetic and real ultrasonic data obtained from artificial defects is used to show the improved performance of the proposed technique over conventional ones, based on second-order statistics (SOS), commonly used in ultrasonic NDE.

## 1. INTRODUCTION

Pulse echo signals measured in ultrasonic NDE include the effects of the measuring systems, the propagation paths taken by the ultrasonic waves, and are corrupted by additive noise. For instance, the ultrasonic signals for a particular reflector recorded under the same conditions, but using different transducers can be quite different. This leads to the difficulty of comparing and analyzing signals particularly in automated defect identification systems using different transducers. Generally, it is assumed that the ultrasonic model is governed by a linear mechanism. Deconvolution operation therefore, seeks to undo the masking effects and extract the defect impulse response which is an essential step for the identification and characterization of defects. Conventional deconvolution techniques such as least squares (LS), Wiener filter, and minimum variance deconvolution (MVD) [1] are sensitive to the additive Gaussian noise and yield a minimum phase defect signature which contradicts the nonminimum phase property of

ultrasonic signals [1]. The paper objective is to formulate the ultrasonic model in HOS domain using cumulants. The processing in HOS domain is more suitable to recover the defect impulse response due to the desirable properties of HOS [3]. Comparison of impulse responses obtained using the proposed HOS-based deconvolution technique and conventional Wiener filter technique demonstrates clearly the superiority of the former technique. In the next section, we present the Wiener filter deconvolution scheme, and show in section III how this scheme can be extended to HOS domain. Simulation results are presented in section IV where it is shown that the proposed method is a good candidate for the deconvolution of NDE signals.

## 2. CONVENTIONAL SOS-BASED DECONVOLUTION METHODS

A measured ultrasonic flaw signal,  $y(k)$ , can be modeled as the convolution of the measurement system impulse response function,  $x(k)$ , with the defect impulse response function,  $h(k)$ , plus noise,  $n(k)$ <sup>1</sup>. The model can be written as:

$$y(k) = x(k) \otimes h(k) + n(k) \quad (1)$$

where  $\otimes$  denotes the linear convolution operator. With this model, defect of a particular geometry would be completely characterized by  $h(k)$ . Many deconvolution techniques, that have been developed in different engineering areas ranging from seismic exploration to medical imaging, can be used to extract  $h(k)$  from Eq. 1. Chen and Sin [1, 2] studied the applicability of existing deconvolution techniques to ultrasonic NDE. Wiener filter method was found to be the most appropriate scheme for the NDE context. Wiener filter requires a-priori knowledge about the noise and the defect scattering amplitude distribution. In practice, information

---

<sup>1</sup>The discrete representation is used throughout the paper.

about the defect scattering amplitude is available only in rare instances [5]. Also, reliable estimates of the noise distribution parameters are generally unavailable in the NDE context. The lack of this a-priori knowledge constitutes a major limitation of Wiener filter method. The HOS formulation will remove this limitation.

### 3. HOS-BASED DECONVOLUTION

Using the HOS properties [3], Eq. 1 can be written in HOS domain as:

$$C_n^y(w_1, \dots, w_{n-1}) = C_n^x(w_1, \dots, w_{n-1}) \cdot H(w_1) \cdots H(w_{n-1}) \cdot H^*(w_1, \dots, w_{n-1}) \quad (2)$$

where  $H(w)$  is the Fourier transform of  $h(k)$ . Eq. 2 can be further reduced to:

$$C_n^y(w_1, \dots, w_{n-1}) = C_n^x(w_1, \dots, w_{n-1}) \cdot C_n^h(w_1, \dots, w_{n-1}) \quad (3)$$

where  $C_n^h(w_1, \dots, w_{n-1})$  is the “polyspectrum” of  $h(k)$ . Only the bispectrum (n=3) is used in this work. For n=3, Eq. 3 is written as:

$$C_3^y(w_1, w_2) = C_3^x(w_1, w_2) \cdot C_3^h(w_1, w_2) \quad (4)$$

It should be noted that  $n(k)$  does not need to be Gaussian, but can have any symmetrical probability density function (PDF). Eq. 4 is used to obtain a high resolution estimate of  $h(k)$ . Details of the estimation procedure are given below.

#### 3.1. Signal Recovery From the Bispectrum

An estimate of  $h(k)$  can be obtained from  $C_3^h(w_1, w_2)$ . The signal (phase) recovery operation requires considerable efforts [3, 6] and a-priori phase information (usually not available). Moreover, the recovered signal is contaminated with an estimation error that can have a high variance [3]. Taking the complex logarithm of Eq. 4 yields the bicepstrum defined by Pan and Nikias [3, 7]:

$$b_3^y(m_1, m_2) = b_3^x(m_1, m_2) + b_3^h(m_1, m_2) \quad (5)$$

$b_3^y(m_1, m_2)$ ,  $b_3^x(m_1, m_2)$  and  $b_3^h(m_1, m_2)$  represent the bicepstrum of  $y(k)$ ,  $x(k)$  and  $h(k)$ , respectively. Based on Eq. 5, we describe in this paper a simple but accurate recovery method. The recovery method is based on the inter-relation between the bicepstra and the bispectra defined by Pan and Nikias [3, 7] as:

$$m_1 \cdot b_3^h(m_1, m_2) = F_2^{-1} \left[ \frac{F_2 \{ \tau_1 \cdot c_3^h(\tau_1, \tau_2) \}}{F_2 \{ c_3^h(\tau_1, \tau_2) \}} \right] \quad (6)$$

where  $F_2[\cdot]$  and  $F_2^{-1}[\cdot]$  denote the 2-dimensional forward and inverse Fourier transforms, respectively.  $c_3^h(\tau_1, \tau_2)$  and  $b_3^h(m_1, m_2)$  are the third-order cumulants and the bicepstrum of  $h(k)$ . Using the properties of the Fourier transform, Eq. 6 can be expressed as:

$$m_1 \cdot b_3^h(m_1, m_2) = F_2^{-1} \left[ \frac{j \cdot \frac{\partial}{\partial w_1} \{ C_3^h(w_1, w_2) \}}{C_3^h(w_1, w_2)} \right] \quad (7)$$

where  $\frac{\partial}{\partial w_1}(\cdot)$  is the partial derivative with respect to  $w_1$  and  $j = \sqrt{-1}$ . Eq. 7 forms the basis of the recovery technique. First, it shows an alternative relationship between the bicepstrum and the bispectrum using the derivative of the logarithm rather than the logarithm relation traditionally used. Second, it does not require any phase unwrapping technique needed by the complex logarithm operation. This enables the recovery method to be highly accurate when compared to other recovery techniques [3, 6].  $h(k)$  is readily estimated from the cepstral parameters  $A^{(m)}$  and  $B^{(m)}$  associated with  $b_3^h(m_1, m_2)$  [3, 7]. The proposed algorithm used to estimate the defect impulse response  $h(k)$  is as follows:

1. Estimate the bispectra of  $x(k)$  and  $y(k)$  using any of the available estimation techniques [3].
2. Use Eq. 7 to estimate the bicepstrum of  $x(k)$  and  $y(k)$ .
3. Calculate the bicepstrum of the defect using Eq. 5.
4. Obtain the bicepstral parameters  $A^{(m)}$  and  $B^{(m)}$  from  $c_3^h(m_1, m_2)$ . Details are given in [3, 7].
5. Use Oppenheim and Schaffer algorithm [4, 7] to compute an estimate of  $h(k)$  from the bicepstral parameters  $A^{(m)}$  and  $B^{(m)}$ .

### 4. SIMULATION AND RESULTS

In this section, we first use synthetic data generated using the model shown in Fig. 1 to test and compare the proposed deconvolution technique with Wiener filter method. Thereafter, real ultrasonic data obtained from artificial defects will be used. The input signal,  $x(k)$ , is taken as a Gaussian pulse that is amplitude modulating a single tone carrier whose frequency lies in the ultrasonic range. The noise,  $n(k)$ , having a normally distributed PDF, is scaled by a factor  $\alpha$  to account for the different SNR levels considered. The defect impulse response,  $h(k)$ , is modeled by the following system who is known to have a maximum phase part, and having a transfer function given by:

$$H(z) = 0.2179z - 0.747 + 0.6085z^{-1} + 0.1533z^{-2}$$

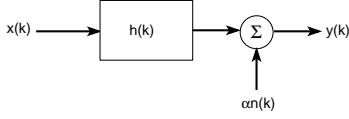


Figure 1: Ultrasonic Defect Model.

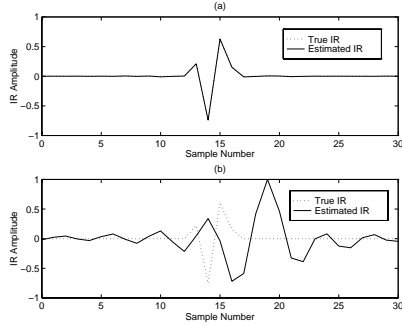


Figure 2: Estimated impulse responses at 40 dB SNR level. HOS-based (a) and Wiener filter (b) methods.

Estimation of  $h(k)$  using  $x(k)$  and  $y(k)$  is carried out using Wiener filter and the proposed technique. The results reported in this paper represent the ensemble average of 50 different runs with data length equal to 1024. Fig. 2(a and b) shows the estimated impulse responses at an SNR level of 40 dB. For comparison, the true impulse response is also displayed. For such a high SNR level, Wiener filter (Fig. 2(b)) method yields a reasonably good estimate as expected. However, for low SNR levels, the obtained estimate deviates considerably from the true one, while the HOS-based method yields a highly accurate estimate. Fig. 3(a and b) illustrates the simulation result at 10 dB SNR level. It is noted, in both cases, that Wiener filter method fails to preserve the nonminimum phase character of the defect impulse response. Next, the performance of the proposed technique is evaluated at different SNR levels. The error norm between the true and estimated

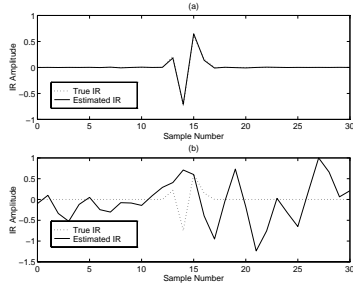


Figure 3: Estimated Impulse responses at 10 dB SNR level. HOS-based (a) and Wiener filter (b) methods.

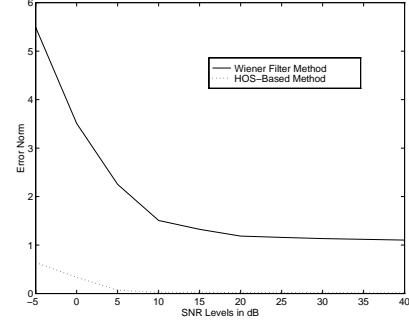


Figure 4: Wiener and HOS-based methods performance versus SNR levels.

impulse responses is computed to quantify the deconvolution performance. Fig. 4 shows the performance of the proposed deconvolution method versus SNR levels in dB. In conformity with theory, the HOS-based deconvolution technique yields accurate and high resolution estimates of  $h(k)$  even at extremely low SNR levels. For comparison, the performance of the Wiener filter is also included. A gain in performance of approximately 30 dB is achieved using the proposed method at the expense of an increased computational complexity [3]. The proposed deconvolution technique is tested using real ultrasonic data [1, 2], which are part of a larger data set obtained from the Army's Material Technology laboratory (Watertown, MA). The ultrasonic signals used are shown in Fig. 5; namely, T15A0, and T15A2. T15A0 (Fig. 5(a)) is the measurement system impulse response, also known as the reference signal, while T15A2 (Fig. 5(b)) is the pulse echo from an angular-cut hole (see [1] for an illustration of the defect geometry). The center frequency of the transducer is 15 MHz, and the A-scan signals contain 512 data points digitized at a sampling rate of 100 MHz. The estimated impulse response of T15A2 defect using the proposed scheme is shown in Fig. 6. The estimated defect signature is characterized by its peak sharpness and high resolution. These features are highly desired in the ultrasonic NDE processing.

## 5. CONCLUSION AND DISCUSSION

For mathematical simplicity, the ultrasonic NDE model is described by a convolutional operation. Extraction of a signal that is insensitive to the noise and the measurement system, but dependent on the defect type only, is the ultimate goal and the challenge for today's NDE Scientific and Engineering communities. As ultrasonic pulse echoes are found to be nonminimum phase systems, and that the acoustic noise due to scattering from the grain inside the propagation media is not neces-

sarily Gaussian, SOS-based deconvolution techniques, being phase blind, cannot therefore, reliably estimate the defect impulse response. In this contribution, we have formulated the defect ultrasonic model in the HOS domain in which the processings are more suitable to easily filter out any additive noise with a symmetrically distributed PDF. Simulation results using synthetic data demonstrate that the proposed deconvolution technique is a good candidate for the extraction of the defect signature from signals with extremely low SNR levels. Real ultrasonic signals are used to extract impulse responses of artificial defects, which are found to be nonminimum phase systems. The estimated defect signatures using the proposed HOS-based method are characterized by their peaks sharpness and high resolution.

## 6. ACKNOWLEDGMENT

The first author would like to acknowledge the support of King Fahd University of Petroleum and Minerals (KFUPM).

## 7. REFERENCES

- [1] S. K. Sin and C. H. Chen, "A Comparison of deconvolution techniques for the ultrasonic nondestructive evaluation of materials," *IEEE Trans. On Image Processing* 1(1):3–10, Jan. 1992.
- [2] C. H. Chen and S. K. Sin, "High resolution deconvolution techniques and their applications in ultrasonic," *Inter. Jour. Of Imag. Sys. and techn.*, 1:223–242. John Wiley and Sons, 1989.
- [3] C. L. Nikias and A. P. Petropulu. *Higher-Order Spectra Analysis : A Nonlinear Signal Processing Framework*. Prentice Hall, Englewood Cliffs, 1993.
- [4] A. V. Oppenheim and R. W. Schaffer. *Discrete-Time Signal Processing*. Prentice Hall, Englewood Cliffs, 1989.
- [5] S. P. Neal and P. L. Speckman and M. A. Enright, "Flaw signature estimation in ultrasonic nondestructive evaluation using Wiener filter with limited prior information," *IEEE Trans. on Ultrason. Ferroelec. And Freq. Contr.* 40(4):347–357, July 1993.
- [6] T. Matsuoka and T. J. Ulrych, "Phase estimation using the bispectrum," *IEEE Proceedings*, 72(10):1403–1411, Oct. 1984.
- [7] R. Pan and C. L. Nikias, "The Complex cepstrum of higher-order cumulants and non minimum phase system identification," *IEEE Trans. on ASSP.*, 36(2):185–205, Feb. 1988.

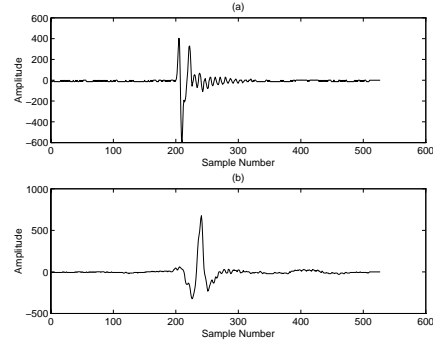


Figure 5: Experimental reference (a) and echo (b) signal of defect A2 at 15 MHz.

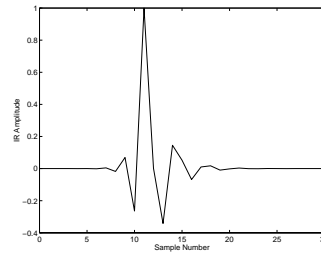


Figure 6: Estimated impulse response of defect T15A2 using the HOS-based method.